Catalysis Today 181 (2012) 102–107

Contents lists available at ScienceDirect

Catalysis Today

journal homepage: www.elsevier.com/locate/cattod

The adsorption of CO on potassium doped molybdenum carbide surface: An ab-initio study

Carolina Pistonesi, María Estela Pronsato, László Bugyi[1], A. Juan*

Departamento de Física, Universidad Nacional del Sur e IFISUR (UNS-CONICET), Av. Alem 1253, (8000) Bahía Blanca, Argentina

ARTICLE INFO

Article history:
Received 26 February 2011
Received in revised form 19 April 2011
Accepted 30 May 2011
Available online 2 July 2011

Keywords:
DFT
Molybdenum carbide
Adsorption
CO
K

ABSTRACT

We have studied the effect of K on the adsorption of CO on the β-Mo_2C (0 0 1) surface with a periodic supercell method using Density Functional Theory calculations, with the PBE functional the generalized gradient approximation. The most favorable sites for CO adsorption are three-fold carbon deficient Mo sites on both clean and K promoted surface. Adsorption is more favorable in the presence of K.

The electronic configuration analysis shows that in all cases the CO molecule withdraws charge from the surface, the larger charge transfer occurs on the K promoted surface.

1. Introduction

It is of great practical interest to replace expensive platinum metals showing unique catalytic activity for heterogeneous reactions in the gas or liquid phase by cheaper but active materials. The first observation regarding that tungsten carbide exhibited platinum-like behavior in surface catalysis [1] initiated broad investigations about the catalytic behavior of the carbides of groups IV–VI early transition metals, often showing catalytic activities similar to those of the Pt-metals [2–4]. There are great efforts to enhance the efficiency of energy production from fossil fuels, which needs finding effective and cheap catalysts for fuel cell application. Potential candidates are tungsten carbides [5] while molybdenum carbides may be active components in composite electrocatalysts [6], ensuring a higher CO-tolerance of platinum in the absence of expensive Ru-additive [7]. Moreover, surface science studies indicated that molybdenum carbides are very active toward the dissociation of methanol and water, suggesting the possibility of using molybdenum carbides as electrocatalytic promoters of tungsten carbides in methanol fuel cells [8].

Mo_2C shows excellent activity and selectivity in many other catalytic processes, especially in hydrodesulphurization (HDS), hydrodenitrogenation (HDN), isomerization of alkanes, CO hydrogenation and the partial oxidation of methane to syngas [4]. It must be emphasized that besides mimicking the behavior of platinum metals, molybdenum carbide catalysts open up new reaction routes. It was found that ZSM-5 supported Mo_2C catalyzed the aromatization of methane [9,10], ethanol [11], methanol [12] and dimethyl ether [13]. Carbon supported molybdenum carbide showed a different reaction route resulting mainly in hydrogen production [14], which could be promoted by potassium [15]. The promoter effect of alkali metals is well documented on transition metals [16], but on transition metal carbides much less work has been done.

The above findings reported in the literature show that molybdenum carbide is an important catalyst in conversion of small hydrocarbon molecules and their derivatives. Since the transformation of these is mostly accompanied by the formation or presence of carbon monoxide, it is necessary to study the interaction of CO with Mo_2C for understanding the elementary processes. The effect of alkali additive on molybdenum carbides is also of interest, since it can influence substantially not only the product distribution of CH_3OH decomposition [15], but that of CO hydrogenation as well [17]. Addition of potassium promoter to β-Mo_2C resulted in remarkable selectivity shift from hydrocarbons to alcohols in the CO hydrogenation reaction [18].

Adsorption of CO on molybdenum carbide has been investigated both experimentally [19–21] and theoretically [22–24]. Experiments revealed molecular CO desorption at TDS peak temperatures

* Corresponding author. Tel.: +54 291 4595101x2800/2811; fax: +54 291 4595142.
E-mail address: cajuan@uns.edu.ar (A. Juan).
[1] Hungarian Academy of Sciences, Reaction Kinetics Research Laboratory, Hungary, Szeged H-6701, Dóm sqr 7. PO Box 168. Tel.: +36 62 544106; fax: +36 62 544106.

0920-5861/$ – see front matter © 2011 Elsevier B.V. All rights reserved.
doi:10.1016/j.cattod.2011.05.035

of T_p = 325–360 K [20] and T_p = 330 K [21], while recombination of C and O atoms arising from the dissociation of CO gave TDS peaks at 970 K and 1200 K, respectively. On annealing the CO-saturated molybdenum carbide [21], the vibration modes characteristic for molecularly adsorbed CO was strongly suppressed at 300–355 K, indicating the decomposition and desorption of molecule. The effect of potassium depended on the alkali coverage. At low coverage (0.12 monolayer), where K was ionic as shown by work function data, the molecular and associative desorption changed only slightly [21]. At intermediate coverage (0.8 monolayer), the more metallic K stabilized and activated the adsorbed carbon monoxide to such an extent that most of the CO underwent dissociation instead of desorption.

Density functional theory (DFT) is employed to trace the CO interactions with a Mo-terminated β-Mo_2C surface and to discuss the electronic consequences of doping the surface with K. The theory and model are considered in the next sections.

2. Computational method and adsorption model

In the present work, calculations were performed using DFT implemented in the Vienna Ab-initio Simulation Package (VASP 5.2 version) which uses a plane-wave basis and a periodic supercell method [25–28]. The electron projector augmented wave (PAW) method was employed [29], and the generalized gradient approximation (GGA) with the Perdew–Burke–Ernzerhof (PBE) functional were used [30,31]. Geometry optimizations were obtained by minimizing the total energy of the unit cell using a conjugated-gradient algorithm to relax the ions [32]. The electronic charges on atoms were computed using Bader analysis [33].

The β-Mo_2C phase has a crystal structure with Mo atoms slightly distorted from their positions in closed-packed planes and carbon atoms occupying one-half of the octahedral interstitial sites. The structure of β-Mo_2C (0 0 1) surface includes a series of alternating Mo and C layers. The calculated DFT lattice parameters for the bulk β-Mo_2C are a = 5.273 Å, b = 6.029 Å, c = 4.775 Å which were obtained by bulk optimization in a previous study [34]. We modeled the surface with a slab of four-layer thickness (two layers of Mo atoms and two layers of C atoms) and each slab has two formula unit cells width, resulting in a 6.0 Å by 10.8 Å surface with a thickness of 4.8 Å. The vacuum spacing between two repeated slabs was 11.8 Å. During optimization the first two layers were allowed to relax, and a set of 3 × 3 × 1 Monkhorst-Pack k-points was used to sample the Brillouin Zone. For adsorption calculations the adsorbed species and the first two surface layers were allowed to relax. It was used a kinetic energy cutoff of 750 eV for all the calculations, which converges the total energy to ∼1 meV/atom for the primitive cell of bulk β-Mo_2C.

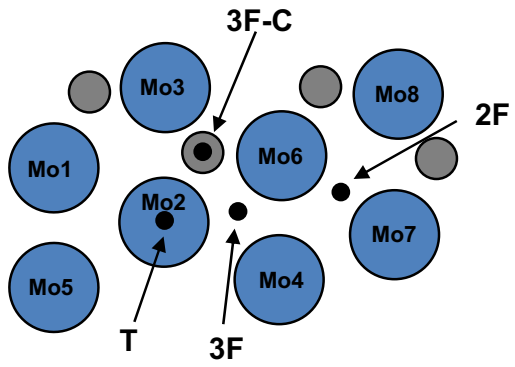

Fig. 2. Position of the selected adsorption sites. Surface Mo atoms (blue), and subsurface C atoms (gray) are indicated.

The CO adsorption energy was computed by subtracting the energies of the gas-phase and surface species from the energy of the adsorbed system as follows

$$E_{ads}(CO) = E\left(\frac{CO}{slab}\right) - E(CO_{gas}) - E(slab)$$

With this definition, negative adsorption energy corresponds to an energetically favorable adsorption site on the surface and more negative values correspond to stronger adsorption bonds, i.e. to higher adsorption energies.

Location of potassium was also considered on the surface at three fold positions. The adsorption energy was −2.19 eV, similar value was reported by Xu using DFT calculations [35]. Experimental finding [21] also indicated an adsorption energy close to this value as suggested by the high desorption peak temperature of ∼900 K for potassium at the zero coverage limit. During optimization for both clean and K promoted surface, first Mo and subsurface C layers and K were allowed to fully relax, while the other two layers were kept frozen. Details of bulk and surface optimization are reported in a previous paper [34]. The unit cell for K-promoted surface is shown in Fig. 1. The optimized K–Mo and K-surface distances were 3.6 Å and 3.06 Å respectively.

The adsorption of the CO molecule was investigated on different sites on Mo terminated Mo_2C surface (see Fig. 2), with CO coordinated via the C atom to the substrate.

In one case CO was placed on a three fold Mo site (formed with Mo3, Mo2 and Mo6) with the underlying C atom of the second surface layer (3F–C). The other case corresponds to CO on a three-fold site without the underlying C atom (3F, formed by Mo2, Mo4 and Mo6). Two fold and top adsorption sites were also considered (2F, and T, respectively).

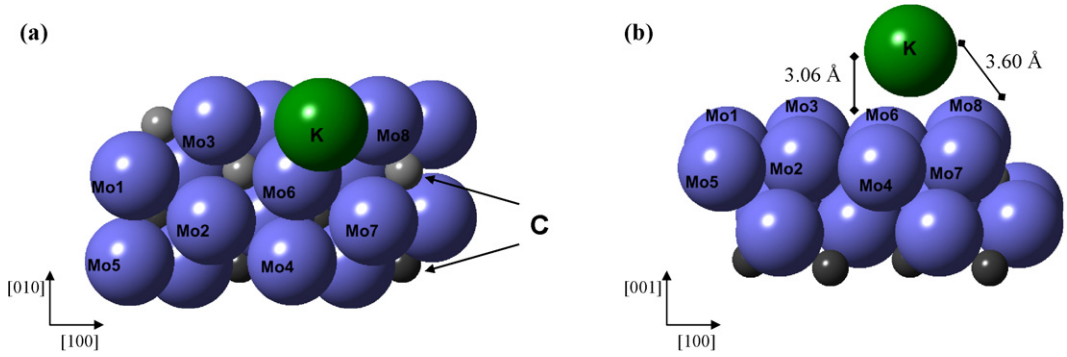

Fig. 1. Surface structure of K adsorption on Mo-terminated Mo_2C surface, top (a) and side (b) view.

Table 1
Calculated CO adsorption energies and geometric parameters for different sites on clean surface.

Site	E_{ads} (eV)	C–O distance (Å)*	C–Mo distance (Å)
3F–C	−1.55	1.20	2.38–2.47–2.68
2F	−2.02	1.19	2.33–2.43
3F	−2.07	1.20	2.03–2.51–2.61
T	−2.03	1.17	2.01

* CO gas phase bond length: 1.14 Å (VASP); experimental: 1.13 Å [42].

In all cases the adsorbate and the first two layers of the slab were fully relaxed. The calculated CO vibrational frequencies were all real, showing that the geometries are in true minima and not on the transition state.

Table 2
Net charges for specific atoms on the surface and on isolated and adsorbed CO.

	Clean surface	Isolated CO	CO/Top	CO/3F
C	–	1.79	1.522	1.180
O	–	−1.79	−1.929	−1.900
q_{CO}	–	0	−0.407	−0.720
Mo1	0.535	–	0.734	0.549
Mo2	0.225	–	0.289	0.379
Mo3	0.538	–	0.591	0.614
Mo4	0.226	–	0.225	0.491
Mo5	0.232	–	0.303	0.242
Mo6	0.532	–	0.541	0.752
Mo7	0.230	–	0.264	0.261
Mo8	0.547	–	0.5824	0.542

*Atom labels are indicated in Fig. 1.

3. Results

The calculated adsorption energies and selected equilibrium distances for the CO adsorbed on the clean Mo-terminated surface are presented in Table 1.

The sites 3F, 2F and T have similar adsorption energies suggesting a stronger bonding to the surface than on the 3F–C site, with C atom underlying. According to our calculation the CO molecule will preferentially adsorb on carbon-deficient sites on the Mo_2C (0 0 1) surface. This finding is in agreement with Monte Carlo simulation results of Nagai et al. [22]. The C–O distance increases after adsorption being larger for the 3F case. Also, the 2F and top sites were found to be energetically slightly less favorable. Similar results were reported by Shi et al. [24].

Fig. 3 shows schematic views of the CO adsorbed on the 3F site (formed by Mo2, Mo4 and Mo6). This is a tilted configuration (60.4°) and is shifted towards Mo4 from the exact position of the 3F site. If we consider the adsorption on the geometric center of the 3F site and without a tilt, the adsorption energy is reduced (−1.85 eV). The CO molecule on the 3F–C is less tilted while on top and 2F sites it is not tilted. These results are in agreement with theoretical results obtained by Tominaga and Nagai [23]. Supposing a non-activated adsorption of CO, the ∼−2 eV adsorption energy for reversibly adsorbed CO (Table 1) would correspond to desorption peak temperature of around 770 K what is considerably higher than those found experimentally at 330 K [20,21] and 450 K [21]. Accordingly, the strongly bound CO state, the presence of which is indicated by calculations must follow another reaction route instead of desorption, namely dissociation. Decomposition of CO on molybdenum carbide occurs at as low temperature as 300–350 K [21], leaving adsorbed C and O atoms on the surface which can decrease the adsorption bond strength of intact CO molecules considerably, resulting in molecular CO desorption with T_p = 350 K and 450 K. These findings underline the fact that catalytically active surfaces may be strongly modified by the reactants or products under real catalytic conditions. To reproduce the low temperature molecular CO desorption states by computer simulation, it will be necessary to take into account the presence of mixed carbon and oxygen adlayer.

Table 2 presents the computed electronic charges for the atoms on the clean surface and the CO molecule when it is adsorbed on top and on 3F sites. Charges are expressed in electron charge units. In both cases there is a decrease on the charge of surface Mo atoms, mainly on those closer to CO (an increase in the positive charge means a decrease on the electron density). When CO is adsorbed on top on Mo1 the electron charge of Mo1 changes from 0.535 to 0.734, decreasing its electronic charge by 0.199. As a result, the surface transfers charge to the CO molecule making it negatively charged with a net charge of −0.407. When CO is adsorbed on the 3F site formed by Mo2, Mo4 and Mo6, its electron density increases mainly from three (instead of one) Mo atoms. The most affected one is Mo4, the closest Mo atom to CO (Mo4-C distance: 2.03 Å), which reduces its charge by 0.265. In the case of a CO adsorption on a 3F site, the net charge transfer to the molecule is higher (−0.720) than on the top site.

The adsorption of the CO molecule was also investigated on potassium promoted Mo_2C surface. Several adsorption sites were considered. In all cases the adsorbate, the first two layers of the slab and the K adlayer were fully relaxed. The most favorable adsorption site is shown in Fig. 4 and corresponds to a 3F site first neighbor to the potassium atom. In this site the CO is tilted with an angle of 69.2° and the K atom is moved away 0.65 Å from its original location. The adsorption energy is −2.403 eV, corresponding to a stronger adsorption as compared with the clean surface and to an even larger stretch of the molecule. The C–O distance increases to 1.24 Å. The final K–O distance is 2.73 Å which is close to the sum of K^+ and O^{2-} atomic radii [36], also the K–O distance in crystalline K_2O obtained by DFT calculations is 2.787 Å [37]. Xu et al. found

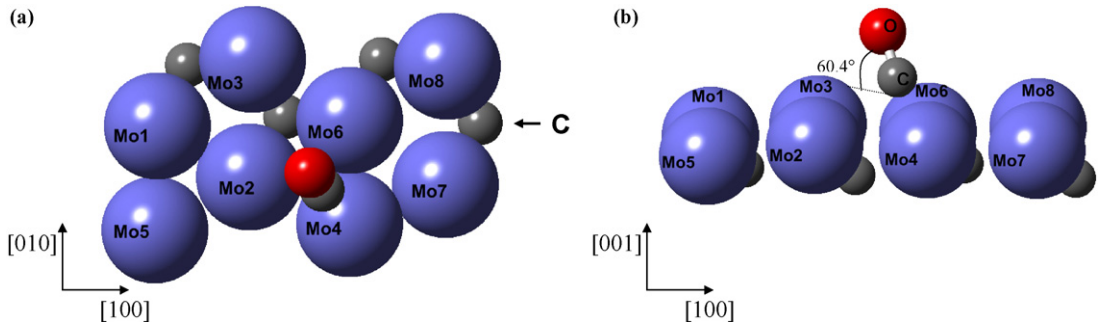

Fig. 3. Surface structure of CO adsorption on Mo-terminated Mo_2C (0 0 1) surface, top (a) and side (b) view. For clarity, not all the surface is shown and only the first two layers are included.

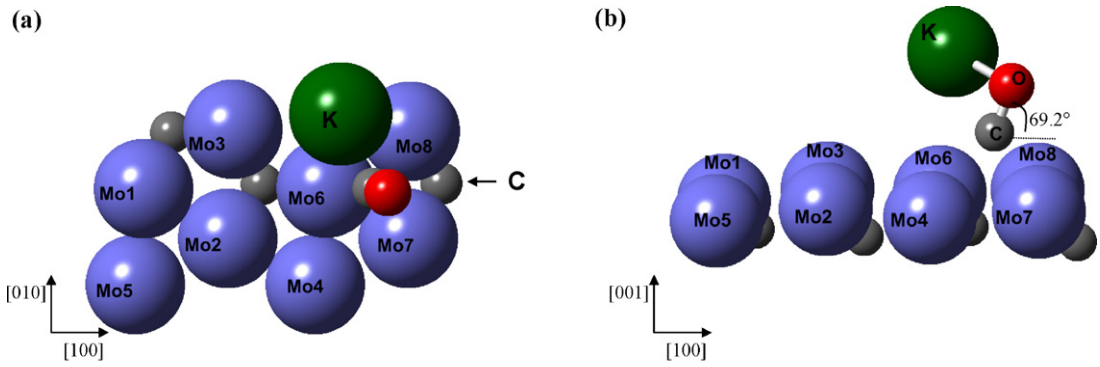

Fig. 4. Top (a) and side (b) view of the surface structure of CO on clean K promoted Mo_2C on a three fold site.

that K has a tendency to abstract oxygen preadsorbed on Rh(1 1 0) to form K–O units [35].

The next stable site in order of energy corresponds to a 3F site second neighbor to K (formed by Mo2, Mo4 and Mo6), for which the adsorption energy is −2.33 eV, (C–O, and K–O distances are 1.22 Å and 3.44 Å respectively). Finally, the third place in energy corresponds to a top site close to K (Mo3) with adsorption energy of −2.21 eV.

Table 3 shows the computed charges for the potassium promoted surface and the CO molecule before and after adsorption on the sites previously mentioned. Let us first analyze the effect of K addition on the isolated surface (before CO adsorption). The comparison of the first column of Tables 2 and 3, shows that on surface Mo atoms the electron density increases due to charge transfer from K mainly to its first neighbors (Mo4, Mo6 and Mo8), while K becomes positively charged. Similar effect of K charge transfer to the surface has been presented in the literature [35,38].

Considering CO adsorption at top positions (Table 3), we can see that Mo atoms being first neighbors to CO show a higher decrease in their charge, specifically Mo3 reduces its charge by 0.237. After adsorption, K also shows a small reduction in its charge. CO becomes more negatively charged on the K-doped surface with a charge of −0.556 (instead of −0.407 on the clean surface). The CO bond length increases slightly to 1.182 Å.

When CO is adsorbed on the 3F site closer to K atom, Mo6, Mo7 and Mo8 reduce their charge by 0.364, 0.236 and 0.262 e respectively, consequently the electron transfer to CO is even larger, resulting in a net charge on the molecule of −1.050 (instead of −0.720 on the clean surface). The CO bond length increases to 1.24 Å. In the case of the 3F site second neighbor to K, the CO charge is −0.941 while the bond length is 1.220 Å.

We have also computed the atom projected density of states (PDOS) by projection of the one-electron wave functions onto atomic Bader volumes (Fig. 5). PDOS on surface Mo and subsurface C atoms of the clean Mo_2C surface is presented in Fig. 5a. The peaks around −12 and −10 eV can be attributed mainly to C s-orbitals, while the band between −6 and 2 eV is mainly Mo d-band interacting with C p-band on its lower energy part (between −6 and −4 eV). There is also a strong peak at −27 eV from Mo p-orbitals (out of scale on these figures) which is not relevant for the present analysis. Kitchin et al. [39] reported similar bands associated with hybridization between d-orbitals and the carbon s–p orbitals.

In the case of CO adsorption, we have projected the sum over all atomic orbitals of C (CO) and O (CO). Fig. 5b shows PDOS on the adsorbed CO molecule and surface Mo bonded to CO and subsurface C atoms. CO contributes with new states mainly in the low part of the band from −6 to −7 eV. There is also a peak around −9 eV and also a small peak near −23 eV (from the C atom of the CO).

When CO is adsorbed on the K promoted surface (Fig. 5c), PDOS curves show that the peaks around −6 and −9 eV are slightly shifted towards lower energy values. This corresponds to a stabilization of the electron states of the CO molecule, which is in agreement with the increment on the adsorption energy. The peak at −15 eV corresponds to strongly localized K 3p states and do not overlap with Mo_2C states. This agrees with previous finding that the adsorption of alkali metals do not affect the transition metal d band [40,41].

Finally we analyzed the effect of a higher K coverage having 3K atoms on the surface of the unit cell. Table 4 summarizes CO adsorption energies and distances for minima energy configurations. The

Table 4
CO adsorption energies and geometric parameters for different adsorption sites on K promoted surface.

	Mo_2C	K–Mo_2C	3K-Mo_2C
E_{ads} (3F site) (eV)	−2.07	−2.40 (−2.33)*	−2.82 (−2.64)*
d C–O (3F) (Å)	1.198	1.240	1.280
E_{ads} (top site) (eV)	−2.03	−2.20	−2.56
d C–O (top site) (Å)	1.168	1.182	1.240

* Corresponds to a three-fold site second neighbor to K.

Table 3
Net charges for specific atoms on K-Mo_2C surface and on isolated and adsorbed CO.

	K/Mo_2C	Isolated CO	Top	3F (K 2nd neighbor)	3F (K 1st neighbor)
C	–	1.79	1.394	1.019	0.914
O	–	−1.79	−1.950	−1.961	1.962
q_{CO}	–	0	−0.556	−0.941	−1.050
Mo2	0.213		0.300	0.379	0.219
Mo3	0.488		0.725	0.582	0.500
Mo4	0.089		0.174	0.483	0.110
Mo6	0.374		0.423	0.621	0.738
Mo7	0.156		0.165	0.201	0.392
Mo8	0.397		0.573	0.529	0.659
K	0.774		0.810	0.823	0.854

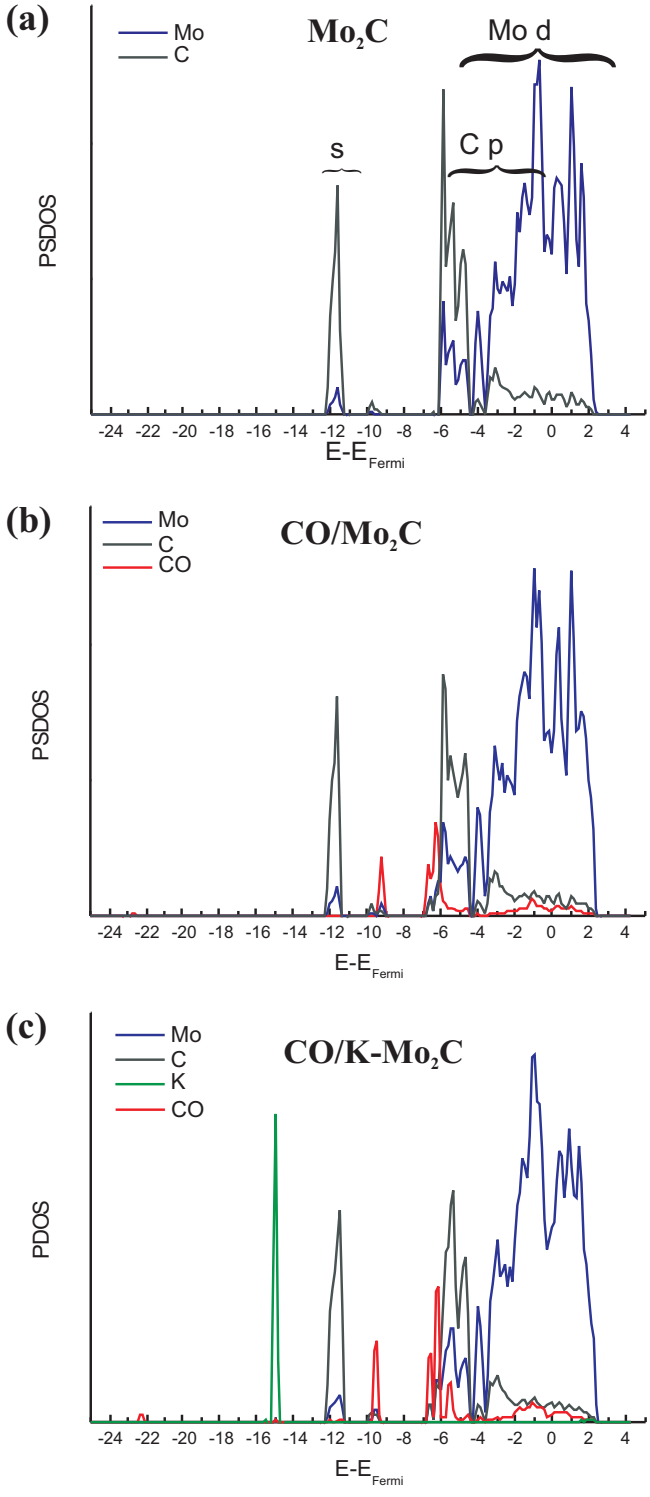

Fig. 5. PDOS on Mo and C surface atoms for the Mo-terminated surface (a), PDOS on Mo and C surface atoms and the CO adsorbed molecule on the clean surface (b), PDOS on Mo, C and K surface atoms and the CO adsorbed molecule on the K doped surface (c).

adsorption energy of CO and the C–O bond length both increase with K content. Adsorption sites close to K atom are energetically the most favorable ones.

Table 5 shows the calculated stretching frequencies of the CO molecule. The stretching vibration mode for the isolated molecule is 2119 cm^{-1}. Preadsorbed K produces a shift to lower frequency values. The CO bond is elongated and possibly weakened, giving rise to lower stretching frequencies. This is a well-known decrease of stretching frequencies as shown in [16]. Comparison of present calculated frequencies with experimental data for CO adsorbed on K-modified molybdenum carbide surfaces [21] can be done at the low CO coverage limit and good agreement is found; at high potassium coverage frequencies of 1340 cm^{-1} and 1282 cm^{-1} were calculated (Table 5) and a loss at around 1305 cm^{-1} was measured. Difference between calculated and measured frequencies appear in the 1750–1930 cm^{-1} region; calculation gives adsorption states characterized by these frequencies on K-free surfaces, but no peaks were detected by HREELS on CO-covered Mo(1 0 0)/Mo_2C surface in this region. The difference can be rationalized if we take into account that the present calculations are made for Mo-terminated surface while the surface of Mo(1 0 0)/Mo_2C sample [21] was composed of both C and Mo atoms, showing less electron sending propensity to elongate C–O bond. In contrast to this, on the p(4 × 4)–C/Mo(1 1 0) surface [19] loss features were detected at ~1600 cm^{-1} and 1845 cm^{-1} at the low CO coverage limit at 140 K, in harmony with the higher reactivity of this surface towards CO.

Table 5
Stretching Frequencies (2119 cm^{-1} for isolated CO).

	Mo_2C	K–Mo_2C	3K–Mo_2C
3F	1747	1613 (1512)*	1340
Top	1926	1847	1282

* Correspond to a 3F site first neighbour to K atom.

4. Conclusions

The adsorption of CO on clean and K promoted Mo-terminated β-Mo_2C (0 0 1) surfaces were computed using periodic DFT calculations. CO adsorbs preferentially on 3-fold carbon deficient Mo sites of the surface.

The adsorption of CO is energetically more favorable in the presence of K preadsorbed on the surface. The lowest energy adsorption sites are those close to K atom.

With the increase of K coverage CO binds more strongly to the surface, C–O distance increases, and the calculated stretching frequencies decrease.

In all cases the CO molecule withdraws charge from the surface, being more extended on the K promoted surface.

Acknowledgements

The authors are grateful for the financial support from PIP-CONICET 2009, SGCyT-UNS, PICTR 656, PICT 1770, and MINCyT-NKTH Cooperation. A.J., C.P and M.E.P. are members of CONICET. We also thank support by Hungarian National Foundation through OTKA K81660.

References

[1] R.B. Levy, M. Boudart, Science 181 (1973) 547–549.
[2] S.T. Oyama (Ed.), The Chemistry of Transition Metal Carbides and Nitrides, Blackie Academic and Professional, Glasgow, 1996, p. 107.
[3] J.G. Chen, Surf. Sci. Rep. 30 (1997) 1–152.
[4] H.H. Hwu, J.G. Chen, Chem. Rev. 105 (2005) 185–212.
[5] H.H. Hwu, J.G. Chen, J. Phys. Chem. B 107 (2003) 2029–2039.
[6] E.C. Weigert, J. South, S.A. Rykov, J.G. Chen, Catal. Today 99 (2005) 285–290.
[7] R. Guil-Lopez, M.V. Martinez-Huerta, O. Guillen-Villafuerte, M.A. Pena, J.L.G. Fierra, E. Pastor, Int. J. Hydrogen Energy 35 (2010) 7881–7888.
[8] H.H. Hwu, J.G. Chen, Surf. Sci. 536 (2003) 75–87.
[9] F. Solymosi, J. Cserényi, A. Szőke, T. Bánsági, A. Oszkó, J. Catal. 165 (1997) 150–161.
[10] D.W. Wang, J.H. Lunsford, M.P. Rosynek, J. Catal. 169 (1997) 347–358.
[11] R. Barthos, A. Széchenyi, F. Solymosi, J. Phys. Chem. B 110 (2006) 21816–21825.
[12] R. Barthos, T. Bánsági, T. Süli Zakar, F. Solymosi, J. Catal. 247 (2007) 368–378.
[13] A. Kecskeméti, R. Barthos, F. Solymosi, J. Catal. 258 (2008) 111–120.
[14] R. Barthos, F. Solymosi, J. Catal. 249 (2007) 289–299.

[15] Á. Koós, R. Barthos, F. Solymosi, J. Phys. Chem. C 112 (2008) 2607–2612.
[16] H.P. Bonzel, Surf. Sci. Rep. 8 (1988) 43–125.
[17] H.C. Woo, K.Y. Park, Y.G. Kim, I.S. Namau, J.S. Chung, J.S. Lee, Appl. Catal. 75 (1991) 267–280.
[18] M. Xiang, D. Li, W. Li, B. Zhong, Y. Sun, Fuel 85 (2006) 2662–2665.
[19] B. Fruhberger, J.G. Chen, Surf. Sci. 342 (1995) 38–46.
[20] J. Wang, M. Castonguay, J. Deng, P.H. McBreen, Surf. Sci. 374 (1997) 197–207.
[21] L. Bugyi, F. Solymosi, J. Phys. Chem. B 105 (2001) 4337–4342.
[22] M. Nagai, H. Tominaga, S. Omi, Langmuir 16 (2000) 10215–10220.
[23] H. Tominaga, M. Nagai, J. Phys. Chem. B 109 (2005) 20415–20423.
[24] X.-R. Shi, J. Wang, K. Hermann, J. Phys. Chem. C 114 (2010) 13630–13641.
[25] G. Kresse, J. Hafner, Phys. Rev. B 47 (1993) 558–561.
[26] G. Kresse, J. Hafner, Phys. Rev. B 49 (1994) 14251–14269.
[27] G. Kresse, J. Furthmüller, Comput. Mater. Sci 6 (1996) 15–50.
[28] G. Kresse, J. Furthmüller, Phys. Rev. B 54 (1996) 11169–11186.
[29] G. Kresse, D. Joubert, Phys. Rev. B 59 (1999) 1758–1775.
[30] J.P. Perdew, K. Burke, M. Ernzerhof, Phys. Rev. Lett. 77 (1996) 3865–3868.
[31] J.P. Perdew, K. Burke, M. Ernzerhof, Phys. Rev. Lett. 78 (1997) 1396–11396.
[32] W.H. Press, B.P. Flannery, S.A. Teukolsky, W.T. Vetterling, Numerical Recipies, Cambridge University Press, New York, 1986, 301.
[33] W. Tang, E. Sanville, G. Henkelman, J. Phys.: Condens. Matter 21 (2009) 84204–84210.
[34] C. Pistonesi, A. Juan, A.P. Farkas, F. Solymosi, Surf. Sci. 602 (2008) 2206–2211.
[35] Y. Xu, H. Marbach, R. Imbihl, I.B. Kevrekidis, M. Mavrikakis, J. Phys. Chem. C 111 (2007) 7446–7455.
[36] 221 L. Pauling, The Nature of the Chemical Bond, third ed., Cornell University Press, Ithaca, NY, 1960, chapter 7.
[37] Y.N. Zhuravlev, N.G. Kravchenco, O.S. Obolonskaya, Russ. J. Phys. Chem. B 4 (2010) 20–28.
[38] P. Mutombo, A.M. Kiss, A. Berko, V. Chab, Nanotechnology 17 (2006) 4112–4116.
[39] J.R. Kitchin, J.K. Norskov, M.A. Barteau, J.G. Chen, Catal. Today 105 (2005) 66–73.
[40] J.J. Mortensen, B. Hammer, J.K. Norskov, Surf. Sci. 414 (1998) 315–329.
[41] S. Gunther, F. Esch, M. Turco, C. Africh, G. Comelli, M. Kiskinova, J. Phys. Chem. B 109 (2005) 11980–11985.
[42] D.R. Lide, in: D.R. Lide (Ed.), CRC Handbook of Chemistry and Physics, 81st ed., CRC Press, Boca Raton, FL, 2000.